

Finite temperature contact for a SU(2) Fermi gas trapped in a 1D harmonic confinement

P. Capuzzi^{1,*} and P. Vignolo^{2,†}

¹*Departamento de Física, Universidad de Buenos Aires, Argentina*

²*Université Côte d'Azur, CNRS, Institut de Physique de Nice,
1361 route des Lucioles 06560 Valbonne, France*

(Dated: December 30, 2021)

We calculate the finite-temperature Tan's contact for N SU(2) fermions, characterized by repulsive contact interaction, trapped in a 1D harmonic confinement within a local density approximation on top of a thermodynamic Bethe Ansatz. The Tan's contact for such a system, as in the homogeneous case, displays a minimum at a very low temperature. By means of an exact canonical ensemble calculation for two fermions, we provide an explicit formula for the contact at very low temperatures that reveals that the minimum is due to the mixing of states with different exchange symmetries. In the unitary regime, this symmetry blending corresponds to a maximal entanglement entropy.

I. INTRODUCTION

The last two-decade progress in the manipulation and detection of ultracold atoms has made this system one of the paradigms for quantum simulators [1, 2]. Indeed, it is possible to deal with bosons and/or fermions, realise low dimensional systems [3, 4], tune interactions by exploiting Feshbach resonances [5], vary the number of spin components [6], and vary the number of particles from many to few [7] down to the two-particle limit [8]. In particular, one-dimensional (1D) Fermi gases are ideal quantum simulators for the exploration of quantum magnetism [6, 9–13]. Recently, it has been shown that the spin-resolved density profiles are not unambiguous observables for the magnetic structure of κ -component 1D SU(κ) fermionic systems [14], while the Tan's contact values for each of the components are [15]. Namely, different symmetry configurations of a quantum many-body state can correspond to the same spin-resolved density profiles, but there is a one-to-one correspondence between each symmetry configuration and its Tan's contact value [15]. Tan's contact is an observable that embeds the information about how particles can approach each other taking into account the presence of all the other particles in the system [16–19]. Therefore, it depends on the number of particles, spin components, interaction strength, temperature and on the external confinement. Unlike the case of 1D homogeneous systems that can be exactly solved [20–22], the 1D harmonically trapped systems, that correspond to the usual experimental situation, cannot be exactly solved for any interaction strength, temperature or number of particles [23–25]. However, one can exploit energy scaling properties in the thermodynamic limit to determine the contact for any (large) number of particles by calculating it for a relative small number of particles. This has been shown for repulsive bosons and multi-component fermions at zero temperature [15, 26–

30], and for Lieb-Liniger bosons at finite temperature [31, 32]. Moreover, for such systems, it has been shown that the finite-interaction contact divided by the contact at the unitary limit, for the same number of particles and temperature, is (almost) a universal function even for a few particles. This means two things: first, that the N -dependency is almost completely contained into the contact calculated at the unitary limit [33, 34], which in turn can be exactly calculated [34–37]; secondly, that a simple two-body calculation at finite interactions and temperature is enough to provide the contact for any number of particles with high accuracy [33, 34].

The study of thermal repulsive multi-component fermions is much more complex than a simple thermal Lieb-Liniger gas. Indeed, the Bethe Ansatz description for the homogeneous system provides an infinite number of coupled equations [38]. At finite temperature, the Lieb-Mattis theorem [39], assuring that the spatial wavefunction for the ground state is the most symmetrical possible, does not hold any more. Different spin states mix and the contact presents a minimum at low, finite temperature that is more pronounced in the strong-interacting limit [40].

In this paper we perform a finite-temperature local density approximation (LDA) on the Bethe Ansatz solution for a SU(2) Fermi gas [40], namely a two-component gas where each component has the same mass and experiences the same external potential, and confirm that the contact presents a well-defined minimum in the trapped gas that is not washed out by inhomogeneity effects. This feature could be observed not only in the momentum distribution tails, but also, for instance, in the behaviours of the pair correlation function and the loss rate in a mixture [41] as a function of the temperature. Furthermore, due to the thermodynamic scaling being independent of particle statistics, the LDA calculation for few fermions provides the contact for any larger number of particles [32]. We compare this LDA result with a simple two-fermion calculation. These two curves give upper and lower bounds for the contact for any N , at corresponding rescaled interaction and temperature [34]. The

* capuzzi@df.uba.ar

† Patrizia.Vignolo@inphyni.cnrs.fr

two-fermion calculation also allows us to enlighten the mechanism underlying the appearance of an exchange symmetry mixing as a function of the temperature. We examine the presence of this thermally driven symmetry blending in two quantities connected to the one-body density matrix: the momentum distribution and the von Neumann entanglement entropy. Comparison with the results for two Lieb-Liniger bosons and for the two non-interacting fermions show that by increasing the temperature, the two-boson momentum distribution hybridize with that of non-interacting fermions. At small interaction strength, we find an analogue behavior for the von Neumann entanglement entropy: for two interacting fermions such an entropy is in between that for two indistinguishable interacting bosons and that for two non-interacting fermions. However, at large interactions, the entanglement entropy for two fermions grows very rapidly with temperature, exceeding the entropy of the two non-interacting fermions. This means that, in the strongly interacting regime, the symmetry blending corresponds to a maximal entanglement entropy, the symmetric and antisymmetric spin configurations becoming energetically equivalent.

The manuscript is organized as follows. The model for the trapped gas is introduced in Sec. II, while its thermodynamical description in the grand canonical ensemble is given in Sec. III. The two-fermion calculation for the contact is detailed in Sec. IV. The momentum distribution and entanglement entropy are discussed in Sec. V. Finally, Sec. VI concludes the manuscript.

II. THE MODEL: THE HARMONICALLY TRAPPED YANG-GAUDIN GAS

We consider a system of N fermions of equal mass m , divided into 2 species with the same population. We assume that the two components are subjected to the same harmonic potential $V(x) = m\omega^2 x^2/2$, and that fermions belonging to different species interact with each other via the contact potential $v(x-x') = g\delta(x-x')$, where g is the interaction strength, and $\delta(x)$ is the Dirac delta function. The total Hamiltonian reads

$$\mathcal{H} = \sum_{i=1}^N \left[-\frac{\hbar^2}{2m} \frac{\partial^2}{\partial x_i^2} + \frac{1}{2} m\omega^2 x_i^2 \right] + g \sum_{i<j} \delta(x_i - x_j). \quad (1)$$

This model is exactly solvable in the absence of harmonic confinement [21, 22, 38], in the Tonks limit $g \rightarrow \infty$ in presence of harmonic confinement [14, 15], or for two particles for any interaction.

III. TAN'S CONTACT FOR N SU(2) FERMIONS

Thermodynamics of the 1D multicomponent Fermi gas with a delta-function interaction is described by an infinite set of coupled equations [38], that thus are numerically difficult to implement. However, for the case of

a SU(2) gas, Pâtu and Klümper [40] have proposed an efficient thermodynamic description that reduces the infinite set to two coupled integral equations. In such a frame, the thermodynamic grand-potential density can be written

$$\Omega_h = -\frac{1}{2\pi\beta} \int dk \left[\ln(1 + e^{-\beta\epsilon_1(k)}) + \ln(1 + e^{-\beta\epsilon_2(k)}) \right] \quad (2)$$

where ϵ_1 and ϵ_2 satisfy the two following coupled integral equations over the wavevector q (with $\alpha \rightarrow 0^+$):

$$\begin{aligned} \epsilon_1(k) &= \frac{\hbar^2 k^2}{2m} - \mu - \frac{c}{2\pi\beta} \int \frac{dq \ln(1 + e^{-\beta\epsilon_2(k)})}{(k-q-i\alpha)(k-q-i\alpha-ic)} \\ \epsilon_2(k) &= \frac{\hbar^2 k^2}{2m} - \mu - \frac{c}{2\pi\beta} \int \frac{dq \ln(1 + e^{-\beta\epsilon_1(k)})}{(k-q+i\alpha)(k-q+i\alpha-ic)} \end{aligned} \quad (3)$$

with $\beta = 1/k_B T$ and $c = mg/\hbar^2$. Pâtu and Klümper have shown that the contact density for the homogeneous system

$$C_h = -\frac{m^2}{\pi\hbar^4} \frac{\partial\Omega_h}{\partial g^{-1}}, \quad (4)$$

exhibits a minimum at a temperature of the order of $T_{0,h} = T_F/\gamma$, $T_F = \pi^2\hbar^2 n^2/(2mk_B)$ being the Fermi temperature, $\gamma = mg/(\hbar^2 n)$ and n the density. For $T \gg T_{0,h}$ the spin degrees of freedom are “disordered” [42], i.e. the different spin states mix together, whereas the density degrees of freedom are unaffected until the temperature becomes of the order of T_F . With the aim to verify if this minimum is not washed out by inhomogeneity in trapped systems, we perform a LDA for the calculation of the contact for the harmonically trapped system. We replace in Eqs. (3) the chemical potential μ with the local value $\mu - m\omega^2 x^2/2$, and obtain a local grand-potential density Ω_x that depends on the position. This approximation is valid in the limit of large interactions $g/(\hbar\omega a_{ho}) \gg 1$ and large number of particles $N \gg 1$. The value of μ for the trapped system is thus obtained by imposing the thermodynamic constraint for an average number of fermions N ,

$$N = - \int dx \frac{\partial\Omega_x}{\partial\mu}. \quad (5)$$

The contact $C_{N,LDA}^{gc}$, in the grand-canonical ensemble, evaluated using the LDA, for a trapped system of an average number of N fermions, can thus be readily calculated as

$$C_{N,LDA}^{gc} = - \int dx \frac{m^2}{\pi\hbar^4} \frac{\partial\Omega_x}{\partial g^{-1}}. \quad (6)$$

It can be easily shown that, as for the case of a bosonic system [32], the contact obeys a scaling law with N

$$\frac{C_{N,LDA}^{gc}}{N^{5/2}} = f(\xi_\gamma, \xi_T) = \tilde{f}(\xi_\gamma, \tau) \quad (7)$$

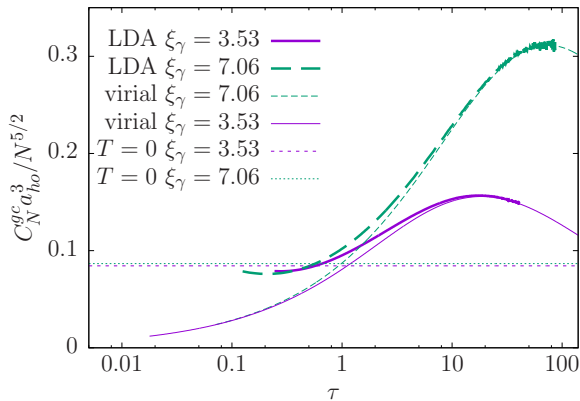


FIG. 1. Rescaled grand-canonical contact $C_N^{gc} a_{ho}^3 / N^{5/2}$ as a function of the reduced temperature τ . Thick lines: LDA calculation, Eq. (6). Thin lines: virial expansion, Eq. (8). Horizontal lines: zero-temperature values [15]. Solid violet curves: $\xi_\gamma = 3.53$. Dashed green curves: $\xi_\gamma = 7.06$.

where f is a universal function of the reduced interaction strength $\xi_\gamma = a_{ho} / (|a_{1D} \sqrt{N}|)$ and of the ratio between the one dimensional scattering length and the de Broglie wavelength $\xi_T = |a_{1D}| / \lambda_T$, \tilde{f} is a universal function of ξ_γ and the reduced temperature $\tau = k_B T / (N \hbar \omega) = 2\pi \xi_T^2 \xi_\gamma^2$. The 1D scattering length is defined by $a_{1D} = -2\hbar^2 / (mg)$ and the de Broglie wavelength by $\lambda_T = \sqrt{2\pi\hbar^2 / (mk_B T)}$. Lengths are measured in units of the harmonic oscillator $a_{ho} = \sqrt{\hbar / m\omega}$. Due to the LDA, the scaling law (7) is expected to be valid in the limit of large N only. In Fig. 1 we show the results for interaction strengths $\xi_\gamma = 3.53$ (solid violet curves) and 7.06 (dashed green curves). The LDA curves are compared with the contact $C_{N, vir}^{gc}$ obtained by means of the virial expansion

$$C_{N, vir}^{gc} = \frac{N^{5/2}}{\pi a_{ho}^3} \frac{\xi_\gamma}{\xi_T} \left(\sqrt{2} - \frac{e^{1/2\pi\xi_T^2}}{\xi_T} \operatorname{erfc}(1/\sqrt{2\pi\xi_T}) \right), \quad (8)$$

that has been obtained analogously to the bosonic case [32]. Eq. (8) is valid in the limit of large interactions ($\xi_\gamma > 1$) and high temperature ($\tau \gg 1$). As for the bosonic case, this function has a maximum at $\xi_T = 0.485$, namely at $\tau = 1.48 \xi_\gamma^2$.

IV. UNDERSTANDING THE CONTACT: TWO-FERMIONS CALCULATION

As pointed out in [40], Eq. (2) is not analytical at $T = 0$ and thus it is not possible to get a Taylor expansion at low temperatures. However, it is possible to obtain an explicit expression of the contact for two fermions in the canonical ensemble from the Helmholtz free energy F . In

this ensemble the contact C_N^c for N particles reads

$$\begin{aligned} C_N^c &= -\frac{m^2}{\pi\hbar^4} \left\langle \frac{\partial F}{\partial g^{-1}} \right\rangle \\ &= -\frac{m^2}{\pi\hbar^4} \frac{\sum_i e^{-\beta E_i} \frac{\partial E_i}{\partial g^{-1}}}{\sum_i e^{-\beta E_i}}. \end{aligned} \quad (9)$$

with $E_i = E_{cm, \ell} + E_{rel, j}$, where only the relative energy $E_{rel, j}$ is a function of g , while the center-of-mass energy $E_{cm, \ell}$ isn't. Aiming at clarifying the different contributions to the energy in the two-fermion calculation, let us first review the case of two trapped Lieb-Liniger bosons [34].

A. Two identical bosons.

For the trapped system composed by two identical bosons interacting through a Dirac delta potential, the spectrum of the relative energy is analytically known [43] and can be written as:

$$E_{rel, i} = \hbar\omega \left(\frac{1}{2} + \nu(i) \right) \quad (10)$$

where $\nu(i)$, with $i \geq 1$, satisfies the relation

$$\frac{\Gamma(-\nu(i)/2)}{\Gamma(-\nu(i)/2 + 1/2)} = f(\nu(i)) = -\frac{2\sqrt{2}}{g} \hbar\omega a_{ho}, \quad (11)$$

where $\Gamma(x)$ is the Gamma function [44]. In the unitary limit $g \rightarrow \infty$, $\nu_\infty(i) = 2i - 1$, where i is a positive integer labelling the levels. This corresponds to the fermionized regime.

The derivative $\partial E_{rel, i} / \partial g^{-1}$ can be written as a function of $f(\nu)$:

$$\frac{\partial E_{rel, i}}{\partial g^{-1}} = -2\sqrt{2} (\hbar\omega)^2 a_{ho} \left(\frac{\partial f}{\partial \nu} \right)^{-1}. \quad (12)$$

Thus the canonical contact for two bosons C_{2b}^c reads

$$\begin{aligned} C_{2b}^c &= \frac{1}{\pi a_{ho}^3} 2\sqrt{2} \frac{\sum_i e^{-\beta\hbar\omega\nu(i)} \left(\frac{\partial f}{\partial \nu} \right)^{-1}_i}{\sum_i e^{-\beta\hbar\omega\nu(i)}} \\ &= \frac{\sum_i e^{-\beta\hbar\omega\nu(i)} C_i}{\sum_i e^{-\beta\hbar\omega\nu(i)}}, \end{aligned} \quad (13)$$

where

$$C_i = \frac{1}{\pi a_{ho}^3} 2\sqrt{2} \left(\frac{\partial f}{\partial \nu} \right)^{-1}_i \quad (14)$$

is the ‘‘zero-temperature contact’’ relative to the energy level i .

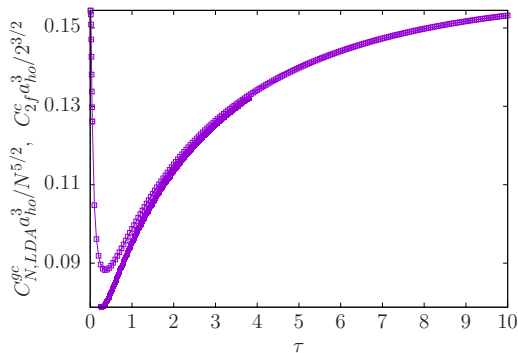


FIG. 2. LDA grand canonical contact $C_{N,LDA}^{gc}$ rescaled by $N^{5/2}$ (full symbols) and the canonical one C_{2f}^c (empty symbols) rescaled by $N^{3/2}(N-1) = 2^{3/2}$ as functions of τ , for the case $\xi_\gamma = 3.53$.

B. Two SU(2) fermions (or bosons).

For the case of two fermions with two spin projections, we have to consider that given that the total wavefunction must be antisymmetric against particle exchange, their spatial part can be either symmetric for the antisymmetric singlet spin state ($s = 0$), or antisymmetric for the symmetric triplet spin state ($s = 1$). The spatially symmetric case is equivalent to the bosonic case, namely $E_{rel,i}^s = E_{rel,i} = \hbar\omega(\nu(i) + 1/2)$ and $C_i^s = C_i$, where C_i has been given in Eq. (14). The antisymmetric case is energetically equivalent to the Tonks limit for bosons where $E_{rel}^a = \hbar\omega(\nu_\infty(i) + 1/2)$, but the contact terms C_i^a are vanishing. Therefore, the canonical contact for two fermions C_{2f}^c reads

$$\begin{aligned} C_{2f}^c &= \frac{\sum_i (e^{-\beta\hbar\omega\nu(i)} C_i^s + e^{-\beta\hbar\omega\nu_\infty(i)} C_i^a)}{\sum_i (e^{-\beta\hbar\omega\nu(i)} + e^{-\beta\hbar\omega\nu_\infty(i)})} \\ &= \frac{\sum_i e^{-\beta\hbar\omega\nu(i)} C_i}{\sum_i (e^{-\beta\hbar\omega\nu(i)} + e^{-\beta\hbar\omega\nu_\infty(i)})}. \end{aligned} \quad (15)$$

At $T = 0$ the fermionic contact coincides with that of two indistinguishable bosons since the ground-state is totally symmetric, while at high temperature the contact is equal to half of the bosonic one since the symmetric and antisymmetric components have almost the same weight. In between these two limits, the contact goes through a minimum as for the thermodynamic limit.

In Fig. 2, we compare the LDA calculation with the exact two-fermion one for the case $\xi_\gamma = 3.53$, by rescaling $C_{N,LDA}^{gc}$ by $N^{5/2}$ and C_{2f}^c by $N^{3/2}(N-1) = 2^{3/2}$, that are the high-temperature grand-canonical and canonical scaling factors for the contact [34]. Indeed, the two curves collapse on the same curve at $\tau \gg 1$. On the other hand, at low temperatures, these two scaling factors do not hold for small number of particles [33, 34] and the two curves stay close but not superposed. However, $C_{N,LDA}^{gc}/N^{5/2}$ and $C_{2f}^c/2^{3/2}$ provide lower and up-

per bounds, respectively for both the rescaled grand-canonical contact $C_N^{gc}/N^{5/2}$ for an average number N of particles and the rescaled canonical one $C_N^c/(N^{3/2}(N-1))$ for N particles [33, 34].

1. $T \simeq 0$ behaviour

From Eq. (15), it is straightforward to show that, at $T = 0$, the two-fermions contact is equal to the two-identical-boson one. On the other hand, at high temperature, the two-fermions contact is about one-half of the bosonic one because the two terms in the denominator are very close. The high temperature regime is marked by $T \gg T_0$, where $T_0 = \hbar\omega[\nu_\infty(1) - \nu(1)]/k_B$ is the difference in the ground-state energy between states with finite and infinite interactions and is the analogue of $T_{0,h}$ for the trapped system. Remark that (see [43]) $[\nu_\infty(i) - \nu(i)] \simeq [\nu_\infty(1) - \nu(1)]$, for any i . In the limit of large interactions

$$k_B T_0 = \hbar\omega[\nu_\infty(1) - \nu(1)] \simeq -\frac{1}{g} \left. \frac{\partial E_{GS}}{\partial g^{-1}} \right|_{g \rightarrow \infty} \simeq \frac{\pi \hbar^4}{m^2} \frac{C_{1,\infty}}{g}, \quad (16)$$

where E_{GS} is the zero temperature ground-state energy of the system, and $C_{1,\infty}$ is the ground-state contact in the unitary limit. In the same limit, one can find a simplified expression for C_{2f}^c at low temperatures as follows

$$\begin{aligned} C_{2f}^c(T \simeq 0) &\simeq \frac{e^{-\beta\hbar\omega\nu(1)} C_1}{e^{-\beta\hbar\omega\nu(1)} + e^{-\beta\hbar\omega\nu_\infty(1)}} \\ &\simeq \frac{C_1}{1 + e^{-\beta\pi\hbar^4 C_{1,\infty}/(gm^2)}}. \end{aligned} \quad (17)$$

Remark that $C_{2f}^c(T \simeq 0)$ is not an analytical function as already pointed out in [40]. In Fig. 3 we show the contact for two SU(2) fermions and one half of the contact of two identical bosons for the cases $g = 20\hbar\omega a_{ho}$ and $g = 10\hbar\omega a_{ho}$. The minimum of the fermionic curves is located at $T = T_{\min} \sim 5T_0$ ($T_0/T_F = 0.037$ for $g = 20\hbar\omega a_{ho}$, and $T_0/T_F = 0.068$ for $g = 10\hbar\omega a_{ho}$).

In the strong interaction regime, $\xi_\gamma > 1$ (large g), the maximum of the contact is located at $\tau = T_{\max}/T_F \simeq 1.48\xi_\gamma^2$ [32]. We can expect that the minimum will disappear when $T_{\min} \simeq T_{\max}$, which thus occurs at $g \simeq 3\hbar\omega a_{ho}$. In Fig. 4 we show the contact for two SU(2) fermions and two identical bosons for the cases $g = 5\hbar\omega a_{ho}$ and $g = 3\hbar\omega a_{ho}$. At $g = 5\hbar\omega a_{ho}$, the minimum and the maximum are close, and they disappear at $g = 3\hbar\omega a_{ho}$, as expected. The fact that the approximated expression (17) works quite well even at intermediate interactions is due to the fact that $C_{1,\infty}/g$ is a good estimate of the difference $\nu_\infty(1) - \nu(1)$ in such a regime too.

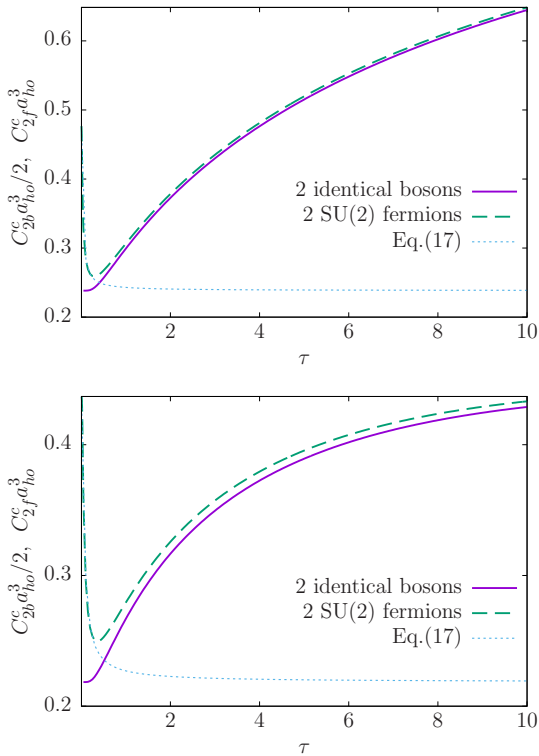


FIG. 3. Two (identical) boson contact $C_{2b}^c/2$ (violet curve) and two SU(2) fermions contact C_{2f}^c (green curve) as a function of τ , for $g = 20\hbar\omega a_{ho}$ (top figure) and $g = 10\hbar\omega a_{ho}$ (bottom figure). The thin blue curve corresponds to Eq. (17).

2. Generalization of Eq. (17)

We now consider a system with N SU(2) fermions. Let C_1 be the zero-temperature contact for the most symmetric state corresponding to a Young tableau with a row of N boxes $\begin{array}{|c|c|c|c|c|} \hline 1 & 2 & 3 & 4 & \dots & N \\ \hline \end{array}$, and \tilde{C}_1 the zero-temperature contact for the state corresponding to a Young tableau with one row with $(N-1)$ boxes and another row with one box $\begin{array}{|c|c|c|c|c|} \hline 1 & 2 & 3 & \dots & N-1 \\ \hline N \\ \hline \end{array}$ [15, 45]. For such a system

$$\begin{aligned} C(T \simeq 0) &\simeq \frac{C_1 + \tilde{C}_1 e^{-\beta\Delta E}}{1 + e^{-\beta\Delta E}} \\ &\simeq \frac{C_1}{1 + e^{-\beta\Delta E}}, \end{aligned} \quad (18)$$

where at the denominator we have neglected the contribution of \tilde{C}_1 which is smaller than C_1 since it corresponds to a less symmetric state. The energy difference ΔE , in the limit of strong interactions, can be written as

$$\Delta E = \frac{\pi\hbar^4}{m^2} \frac{C_{1,\infty} - \tilde{C}_{1,\infty}}{g}. \quad (19)$$

The contact is proportional to the number of pairs that can interact: $N(N-1)/2$ in $C_{1,\infty}$ and $(N-1)(N-2)/2$

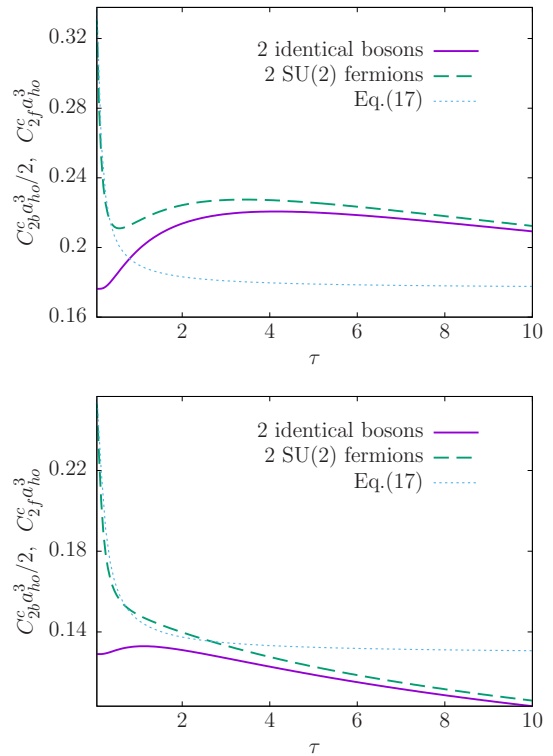


FIG. 4. Two (identical) boson contact $C_{2b}^c/2$ (violet curve) and two SU(2) fermions contact C_{2f}^c (green curve) as a function of τ , for $g = 5\hbar\omega a_{ho}$ (top figure) and $g = 3\hbar\omega a_{ho}$ (bottom figure). The thin blue curve corresponds to Eq. (17).

in $\tilde{C}_{1,\infty}$ (at least in the thermodynamic limit). Thus, one finds that $C_{1,\infty} - \tilde{C}_{1,\infty} \simeq C_{1,\infty} 2/N$. Thus, for the case of N fermions, Eq. (18) takes the form

$$\begin{aligned} C(T \simeq 0) &\simeq \frac{C_1}{1 + e^{-\beta\Delta E}} \\ &\simeq \frac{C_1}{1 + e^{-\beta 2\pi\hbar^4 C_{1,\infty}/(gNm^2)}} \\ &\simeq \frac{C_1}{1 + e^{-\pi C_{1,\infty}/(\tau\xi_\gamma)}} \end{aligned} \quad (20)$$

where $C_{1,\infty} = C_{1,\infty}/(N^{5/2}a_{ho}^3)$ is the rescaled contact. The usual thermodynamical scaling is recovered, since in the thermodynamic limit $C_{1,\infty}$ is a universal function of τ [35].

V. A THERMALLY DRIVEN SYMMETRY BLENDING

The contact behaviour at low temperature is due to the exchange symmetry mixing: at $T = 0$ the only contribution to the contact originates from the fully symmetric ground state, while with increasing the temperature less symmetric states start to contribute and the contact diminishes. The role of less symmetric states is extremely

clear for two fermions where the only possible states are the fully symmetric and the fully antisymmetric with vanishing contact. Aiming at characterizing this symmetry blending process, we have calculated the momentum distribution and the von Neumann entanglement entropy for the two-fermion system. Both quantities can be derived from the canonical one-body density matrix which in turn can be written explicitly.

A. The canonical one-body density matrix

The canonical one-body density-matrix for two fermions reads

$$\rho(x, x') = \frac{\sum_{i,j} e^{-\beta E_{i,j}^s} \rho_s^{i,j}(x, x') + \sum_{i < j} e^{-\beta E_{i,j}^a} \rho_a^{i,j}(x, x')}{\sum_{i,j} e^{-\beta E_{i,j}^s} + \sum_{i < j} e^{-\beta E_{i,j}^a}} \quad (21)$$

where $E_{i,j}^s = E_{cm,i} + E_{rel,j} = \hbar\omega(i + \nu(j))$, $E_{i,j}^a = \hbar\omega(i + j - 1)$, with i and $j \geq 1$. $\rho_s^{i,j}(x, x')$ and $\rho_a^{i,j}(x, x')$ are respectively the exchange symmetric and exchange antisymmetric contributions (see Appendix).

1. The momentum distribution.

The momentum distribution is given by the Fourier transform of the one-body density matrix:

$$n(k) = \frac{1}{2\pi} \int dx \int dx' e^{-ik(x-x')} \rho(x, x'). \quad (22)$$

Analogously to the one-body density matrix, the momentum distribution is a thermally weighted average of the momentum distribution of two Lieb-Liniger bosons and the momentum distribution of two spin-polarized fermions. This is shown in Fig. 5. At very low temperature, $k_B T / (\hbar\omega) = 5 \cdot 10^{-3}$, the fermionic momentum distribution coincides with that for the Lieb-Liniger gas, while as soon as the temperature increases there is a hybridization between the momentum distribution of the Lieb-Liniger gas and the spin-polarized fermionic one.

2. The entanglement entropy.

One may wonder what the occurrence of this symmetry blending means from the quantum information point of view. To answer this question we calculate the von Neumann entanglement entropy,

$$S_e = -\text{tr}[\tilde{\rho} \ln(\tilde{\rho})], \quad (23)$$

where $\tilde{\rho} = \rho(x, x') a_{ho}$. In Fig. 6 we plot S_e for two SU(2) fermions (full symbols) for different interaction strengths: $g/(\hbar\omega a_{ho}) = 100$ (squares), 10 (circles) and 3 (triangles). Each curve has to be compared with the entanglement entropy for two Lieb-Liniger bosons (empty symbols) at

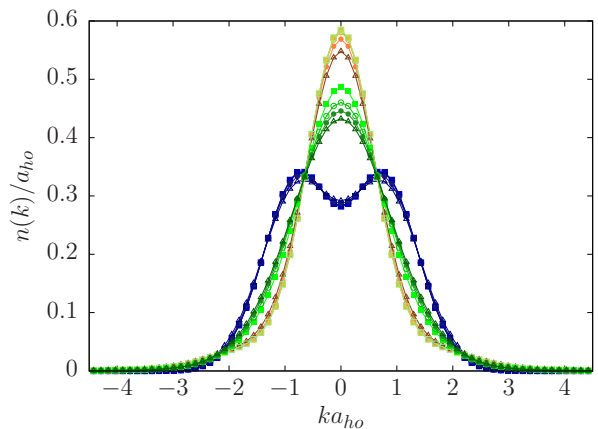


FIG. 5. Two-SU(2)-fermion momentum distribution $n(k)$ (green lines) compared with that for two Lieb-Liniger bosons (yellow lines) and two polarized fermions (blue lines), for $\xi_\gamma = 7.06$, at different temperatures: $\tau = 2.5 \cdot 10^{-3}$ (empty squares), 0.05 (full squares), 0.1 (empty circles), 0.15 (full circles), 0.2 (empty triangles).

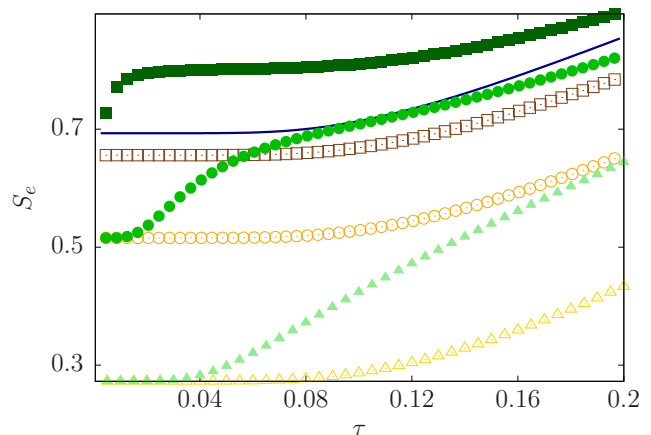


FIG. 6. Von Neumann entanglement entropy S_e as a function of τ for different interaction strengths: $g/(\hbar\omega a_{ho}) = 100$ (squares), 10 (circles) and 3 (triangles). The empty symbols correspond to Lieb-Liniger bosons, while the full symbols correspond to the case of SU(2) fermions. The continuous blue line marks the spin-polarized fermionic case.

the same interaction strength, and with that for two spin-polarized fermions (continuous line).

At small and intermediate interactions, the SU(2) curves are contained between the Lieb-Liniger ones and the spin-polarized one. But, at very large interaction, approaching the Tonks limit, the SU(2) curve overcomes the spin-polarized fermionic one. Indeed, the finite temperature Tonks limit corresponds to a maximal entanglement entropy: the symmetric and the antisymmetric states becoming equiprobable, the two fermions are maximally entangled.

For the spin-polarized case (blue continuous line), we recover at $T = 0$ the well-known limit $S_e = \ln(2) = 0.693$ [46], while there is a sensible effect of the trap in the Tonks limit: in the homogeneous gas it is expected $S_e = \ln(2) - 0.30 = 0.393$ [46], while in the trapped system we find $S_e = \ln(2) - 0.037 = 0.656$ (empty squares). In addition, we find that the sharp increase of the entanglement entropy at low temperature and the minimum of the contact occur simultaneously around a temperature T_0 .

VI. CONCLUSIONS

In this paper we have studied the Tan's contact for N harmonically trapped 1D SU(2) fermions characterized by repulsive contact interactions. By means of a LDA calculation we have verified that the Tan's contact exhibits a minimum at very low temperature as expected in the homogeneous system [40]. With the aim to improve the understanding of the contact minimum, we have calculated the two-fermion contact as well. At $T = 0$ the fermionic contact coincides with that of two indistinguishable bosons since the ground state is totally symmetric, while at high temperature the contact is equal to half of the bosonic one since the symmetric and antisymmetric components have almost the same statistical weight. The minimum, that is a signature of this thermally driven symmetry blending, occurs at an energy scale determined by the energy difference between the ground state and the first excited state. We find that this difference is proportional to the ground-state contact in the large interaction limit. Moreover, we have shown that the symmetry blending, that can be observed in other observables such as the momentum distribution, in the strongly interacting limit, corresponds to a maximal entanglement.

ACKNOWLEDGMENTS

P.V. acknowledges O. Pâtu for very useful exchanges, and F. Chevy, C. Salomon, F. Werner, J. Decamp, M. Albert for useful discussions. The authors also acknowledge A. Minguzzi for her suggestions during the early

stages of this work. This research has been carried out in the International Associated Laboratory (LIA) LI-COQ. P. C. acknowledges partial support from CONICET and Universidad de Buenos Aires through grants PIP 11220150100442CO and UBACyT 20020150100157, respectively.

APPENDIX: THE ONE-BODY DENSITY MATRICES OF TWO PARTICLES

In this section we give some details on the calculation of the one-body density matrices for the antisymmetric and symmetric cases for two SU(2) fermions.

The antisymmetric contribution corresponds to purely noninteracting fermions, and as such the expression for the one-body density matrix is well-known for arbitrary N . For two fermions it can be written as functions of the two occupied single-particle states i and j as

$$\rho_a^{i,j}(x, x') = \frac{1}{2} (\varphi_i(x)\varphi_i(x') + \varphi_j(x)\varphi_j(x')). \quad (24)$$

Given that the total energy for this state is $E_{i,j}^a$, the sum over i, j entering Eq. (21) can be exactly performed in the harmonic confinement case thanks to Mehler's formula [47, 48] which states that

$$\mathcal{K}(x, x', u) \equiv \sum_{n=0}^{\infty} \varphi_n(x)\varphi_n(x')u^n = \frac{1}{\sqrt{\pi(1-u^2)}} \exp \left\{ -\frac{1}{4} \left[\frac{1-u}{1+u}(x+y)^2 + \frac{1+u}{1-u}(x-y)^2 \right] \right\} \quad (25)$$

where $\varphi_n(x) = H_n(x/a_{ho})/\sqrt{a_{ho}2^n n! \sqrt{\pi}} e^{-m\omega x^2/2\hbar}$ is the normalized 1D harmonic oscillator eigenfunction and $|u| < 1$. $H_n(x)$ is the Hermite polynomial of order n . Therefore, summing up the different terms on $\rho_a^{i,j}$ in (21) one finds

$$\sum_{i,j} e^{-\beta E_{i,j}^a} \rho_a^{i,j}(x, x') = \mathcal{K}(x, x', u_\beta) \frac{u_\beta}{1-u_\beta} - \mathcal{K}(x, x', u_\beta^2) u_\beta \quad (26)$$

where $u_\beta = e^{-\beta\hbar\omega}$. This expression allows to obtain an analytical formula for the corresponding density at finite temperature

$$\rho_a(x) = \frac{e^{\beta\hbar\omega} e^{-x^2(\tanh\beta\omega\hbar/2 + \tanh\beta\omega\hbar)}}{2\sqrt{\pi}\sqrt{e^{2\beta\omega\hbar} + 1}} \left\{ e^{\beta\hbar\omega} \sqrt{1 - e^{-4\beta\hbar\omega}} (\cosh(x^2 \tanh\beta\hbar\omega) + \sinh(x^2 \tanh\beta\hbar\omega)) - (e^{\beta\hbar\omega} - 1) \sqrt{1 - e^{-\beta\hbar\omega}} e^{x^2 \tanh\beta\hbar\omega} \right\}. \quad (27)$$

The symmetric contribution to the one-body density

matrix is more involved as it explicitly depends on g

through $\nu(i)$. Nevertheless, the summation over the center-of-mass degrees of freedom can be exactly performed as in the antisymmetric case leading to an expression with a single sum left

$$\sum_{i,j} e^{-\beta E_{i,j}^s} \rho_s^{i,j}(x, x') = \sum e^{-\beta \hbar \omega (1+\nu(i))} \times \int dy \mathcal{K} \left(\frac{x+y}{2a_X}, \frac{x'+y}{2a_X}, u_\beta \right) \phi_i(x-y) \phi_i(x'-y) \quad (28)$$

where

$$\phi_i(x) = \frac{1}{\sqrt{\mathcal{N}_{\nu(i)} a_x}} U \left(-\frac{\nu(i)}{2}, \frac{1}{2}, \frac{x^2}{2a_{ho}^2} \right) e^{-m\omega x^2/4\hbar} \quad (29)$$

is the normalized eigenfunction of the relative motion with energy $\hbar\omega(1/2+\nu(i))$ (c.f. Eq. (10)) and normalizing constant [33]

$$\mathcal{N}_\nu = 2^{-\nu} \Gamma(\nu+1) \sqrt{\pi} \left(1 + \frac{\sin \pi \nu}{2\pi} (\psi(\nu/2+1) - \psi(\nu/2+1/2)) \right). \quad (30)$$

The functions U and ψ are the confluent Hypergeometric function and the digamma function, respectively. Combination of the symmetric and antisymmetric expressions above together with their canonical partition functions allows to efficiently calculate the one-body density matrix for the two fermions, their momentum distribution and von Neumann entropy.

-
- [1] D. Blume, Rep. Prog. Phys. **75** (2012).
- [2] T. Sowinski and M. García-March, Rep. Prog. Phys. **82** (2019).
- [3] H. Moritz, T. Stöferle, M. Köhl, and T. Esslinger, Phys. Rev. Lett. **91**, 250402 (2003), URL <https://link.aps.org/doi/10.1103/PhysRevLett.91.250402>.
- [4] Z. Hadzibabic, P. Kruüger, M. Cheneau, B. Battelier, and J. Dalibard, in *AIP Conference Proceedings* (AIP, Insbruck, Austria, 2006), vol. 869, pp. 155–164, ISBN 9780735403673, ISSN 0094243X, URL <http://aip.scitation.org/doi/abs/10.1063/1.2400645>.
- [5] C. Chin, R. Grimm, P. Julienne, and E. Tiesinga, Rev. Mod. Phys. **82**, 1225 (2010), URL <https://link.aps.org/doi/10.1103/RevModPhys.82.1225>.
- [6] G. Pagano, M. Mancini, P. Lombardi, G. Cappellini, P. Lombardi, K.-J. L. F. Schafer, H. Hu, J. Catani, C. Sias, M. Inguscio, and L. Fallani, Nature Physics **10**, 198–201 (2014).
- [7] A. N. Wenz, G. Zürn, S. Murmann, I. Brouzos, T. Lompe, and S. Jochim, Science **342**, 457 (2013).
- [8] G. Zürn, F. Serwane, T. Lompe, A. N. Wenz, M. G. Ries, J. E. Bohn, and S. Jochim, Phys. Rev. Lett. **108**, 075303 (2012), URL <http://link.aps.org/doi/10.1103/PhysRevLett.108.075303>.
- [9] Y. Liao, A. S. C. Rittner, T. Paprotta, W. Li, G. B. Partridge, R. G. Hulet, S. K. Baur, and E. J. Mueller, Nature (London) **467**, 567 (2010).
- [10] F. Deuretzbacher, D. Becker, J. Bjerlin, S. M. Reimann, and L. Santos, Phys. Rev. A **90**, 013611 (2014), URL <https://link.aps.org/doi/10.1103/PhysRevA.90.013611>.
- [11] S. Murmanna, F. Deuretzbacher, G. Z. urn, J. Bjerlin, S. M. Reimann, L. Santos, T. Lompe, and S. Jochim, Phys. Rev. Lett. **115** (2015).
- [12] W.-B. He, Y.-Y. Chen, S. Zhang, and X.-W. Guan, Phys. Rev. A **94**, 031604 (2016), URL <https://link.aps.org/doi/10.1103/PhysRevA.94.031604>.
- [13] N. Zinner, EPJ Web Conf. **113** (2016).
- [14] J. Decamp, P. Armagnat, B. Fang, M. Albert, A. Minguzzi, and P. Vignolo, New Journal of Physics **18**, 055011 (2016).
- [15] J. Decamp, J. Jünemann, M. Albert, M. Rizzi, A. Minguzzi, and P. Vignolo, Phys. Rev. A **94**, 053614 (2016), URL <https://link.aps.org/doi/10.1103/PhysRevA.94.053614>.
- [16] S. Tan, Ann. Phys. (N.Y.) **323**, 2971 (2008).
- [17] S. Tan, Ann. Phys. (N.Y.) **323**, 2987 (2008).
- [18] S. Tan, Ann. Phys. (N.Y.) **323**, 2952 (2008).
- [19] M. Barth and W. Zwerger, Ann. Phys. **326**, 2544 (2011).
- [20] E. Lieb and W. Liniger, Phys. Rev. **130**, 1605 (1963).
- [21] C. N. Yang, Phys. Rev. Lett. **19**, 1312 (1967), URL <https://link.aps.org/doi/10.1103/PhysRevLett.19.1312>.
- [22] M. Gaudin, Phys. Lett. A **24**, 55 (1967).
- [23] T. Sowinski, T. Grass, O. Dutta, and M. Lewenstein, Phys. Rev. A **88**, 033607 (2013), URL <https://link.aps.org/doi/10.1103/PhysRevA.88.033607>.
- [24] S. E. Gharashi and D. Blume, Phys. Rev. Lett. **111**, 045302 (2013), URL <https://link.aps.org/doi/10.1103/PhysRevLett.111.045302>.
- [25] A. Volosniev, D. Fedorov, A. Jensen, M. Valiente, and N. Zinner, Nat. Comm. **5**, 5300 (2014).
- [26] M. Olshanii and V. Dunjko, Phys. Rev. Lett. **91**, 090401 (2003).
- [27] J. Levinsen, P. Massignan, G. M. Bruun, and M. M. Parish, Science Advances **1**, 1500197 (2015), URL DOI:10.1126/sciadv.1500197.
- [28] S. E. Gharashi, X. Y. Yin, Y. Yan, and D. Blume, Phys. Rev. A **91**, 013620 (2015), URL <https://link.aps.org/doi/10.1103/PhysRevA.91.013620>.
- [29] T. Grining, M. Tomza, M. Lesiuk, M. Przybytek, M. Musiał, R. Moszynski, M. Lewenstein, and P. Massignan, Phys. Rev. A **92**, 061601 (2015), URL <http://link.aps.org/doi/10.1103/PhysRevA.92.061601>.
- [30] N. Matveeva and G. Astrakharchik, New Journal of Physics **18**, 065009 (2016).

- [31] W. Xu and M. Rigol, Phys. Rev. A **92**, 063623 (2015), URL <https://link.aps.org/doi/10.1103/PhysRevA.92.063623>.
- [32] H. Yao, D. Clément, A. Minguzzi, P. Vignolo, and L. Sanchez-Palencia, Phys. Rev. Lett. **121**, 220402 (2018), URL <https://link.aps.org/doi/10.1103/PhysRevLett.121.220402>.
- [33] M. Rizzi, C. Miniatura, A. Minguzzi, and P. Vignolo, Phys. Rev. A **98**, 043607 (2018), URL <https://link.aps.org/doi/10.1103/PhysRevA.98.043607>.
- [34] F. T. Sant'Ana, F. Hébert, V. G. Rousseau, M. Albert, and P. Vignolo, Phys. Rev. A **100**, 063608 (2019), URL <https://link.aps.org/doi/10.1103/PhysRevA.100.063608>.
- [35] P. Vignolo and A. Minguzzi, Phys. Rev. Lett. **110**, 020403 (2013), URL <http://link.aps.org/doi/10.1103/PhysRevLett.110.020403>.
- [36] Y. Yan and D. Blume, Phys. Rev. A **88**, 023616 (2013), URL <https://link.aps.org/doi/10.1103/PhysRevA.88.023616>.
- [37] Y. Yan and D. Blume, Phys. Rev. A **90**, 013620 (2014), URL <https://link.aps.org/doi/10.1103/PhysRevA.90.013620>.
- [38] P. Schlottmann, Journal of Physics: Condensed Matter **5**, 5869 (1993).
- [39] E. Lieb and D. Mattis, Phys. Rev. **125**, 164 (1962), URL <http://link.aps.org/doi/10.1103/PhysRev.125.164>.
- [40] O. I. Pătu and A. Klümper, Phys. Rev. A **93**, 033616 (2016), URL <https://link.aps.org/doi/10.1103/PhysRevA.93.033616>.
- [41] S. Laurent, M. Pierce, M. Delehay, T. Yefsah, F. Chevy, and C. Salomon, Phys. Rev. Lett. **118**, 103403 (2017), URL <https://link.aps.org/doi/10.1103/PhysRevLett.118.103403>.
- [42] V. V. Cheianov, H. Smith, and M. B. Zvonarev, Phys. Rev. A **71**, 033610 (2005), URL <https://link.aps.org/doi/10.1103/PhysRevA.71.033610>.
- [43] T. Busch, B.-G. Englert, K. Rzazewski, and M. Wilkens, Found. Phys. **28**, 549 (1998).
- [44] I. Gradshteyn and I. Ryzhik, *Table of Integrals, Series, and Products* (Elsevier, Amsterdam, 1996).
- [45] M. Hamermesh, *Group theory and its applications to physical problems* (Dover, New York, 1989).
- [46] R. Santachiara, F. Stauffer, and D. C. Cabra, J. Stat. Mech. **05**, L05003 (2007).
- [47] D. Foata, J. Comb. Theory, Ser. A **24**, 367 (1978), ISSN 00973165, URL <https://linkinghub.elsevier.com/retrieve/pii/00973165789006>.
- [48] G. N. Watson, J. London Math. Soc. **s1-8**, 194 (1933), ISSN 00246107, URL <http://doi.wiley.com/10.1112/jlms/s1-8.3.194>.